Proceedings of ASME Turbo Expo 2011
GT2011
June 6-10, 2011, Vancouver, British Columbia, Canada

GT2011-45527

REAL-TIME SIMULATION OF AN EXPERIMENTAL RIG WITH PRESSURIZED SOFC

Paolo Pezzini paolo.pezzini@unige.it
Francesco Caratozzolo francesco.caratozzolo@unige.it
Alberto Traverso alberto.traverso@unige.it

Thermochemical Power Group (TPG) – DiMSET, University of Genoa, Genova, Italy

ABSTRACT

The availability of reliable simulation models can reduce the time required for commissioning test rigs as well as preventing components from suffering serious damage during testing. The aim of this study is to set up and validate, against experimental data, a real-time model referring to the Rolls-Royce Fuel Cell System Limited (RRFCS) hybrid system concept, based on SOFCs. The dynamic model of the SOFC "block" has been developed, run in real-time, and successfully validated against experiments.
Initially, the dynamic evolution of the model is considered under constant inputs at steady-state and is compared against experimental data; secondly, transient behaviour is also considered. Step variations of the main air flow, main fuel flow, syngas flow and electrical current were performed.
The model can now be employed to carry out the following: performance analysis, design verification, development of control strategies, on-line analysis and integration with Human Machine Interface.

NOMENCLATURE

A, B	coefficients in Eqs. 2-4	[ohm, K]
c_p	specific heat at constant pressure	[J kg^{-1} K^{-1}]
ΔH	heat of reaction	[MJ kmol^{-1}]
ΔG	Gibbs free energy change	[J mol^{-1}]
ΔG^0	std Gibbs free energy change	[J mol^{-1}]
D_1, D_2	coefficients	[A]
Q	heat flow	[W]
d_t	sample time	[s]
E	activation energy	[J mol^{-1}]
F	Faraday constant	[C mol^{-1}]
h	convective coefficient	[W m^{-2} K^{-1}]
h_d	equivalent hydraulic diameter	[m]
I	electrical current	[A]
L	cell length	[m]
LHV	Lower Heating Value	[kJ kg^{-1}]
$K_{p,ref}$	equilibrium constant	[Pa^2]
$K_{p,\ shift}$	equilibrium constant	
k	air thermal conductivity	[W m^{-1} K^{-1}]
$\dot{m}$	mass flow rate	[kg s^{-1}]
M	mass	[kg]
N	molar flow rate	[mol s^{-1}]
Nu	Nusselt number	
p	pressure, partial pressure	[10^5 Pa]
P^0	reference pressure	
r	reaction rate	[mol m^{-3} s^{-1}]
R_g	specific gas constant	[J mol^{-1} K^{-1}]
S	heat exchange surface	[m^2]
T	temperature	[K]
t	time	[s]
V	potential	[V]
V_{oc}	thermodynamic open circuit electrical potential	[V]

Greek Letters

υ	stoichiometric coefficient	
Ω	electrical resistance	[ohm]
ρ	electrical resistivity	[ohm^{-1}]
Δ	variation term	

Subscripts

a, c, el	anode, cathode, electrolyte
act	activation
av	average
dif	diffusion
k	chemical reaction
sol	solid
ref	reference
re	reformer
t	total

Acronyms

RRFCS	Rolls-Royce Fuel Cell System Limited
TPG	Thermochemical Power Group
OGB	Off Gas Burner

INTRODUCTION

In the framework of system modelling and simulation, real-time models play an important role because of their suitability for tuning controllers and hardware in-the-loop implementation [1][2][3][4].
The integrated SOFC-GT hybrid system layout, being targeted by RRFCS (not yet available at full scale for testing), is made of four 250kW units called Generator Module (GM). Each GM is a virtually stand-alone unit capable of operating on its own and sharing a limited number of auxiliaries with the other GMs of the 1 MW package [5][6]. Each GM consists of a two stage turbogenerator coupled with pressure vessels containing sub-systems called tiers; tiers contain the cathode ejector, anode ejector and off-gas burner, fuel cell stack and internal reformer are arranged into a number of inner "blocks".
Dynamic simulation models are fundamental for the initial development of control strategies and trial-and-error "virtual" experimentation [7][8].
In this respect, the real-time model developed and validated in this study was subject to three main requirements: modularity, flexibility and real-time execution. The modular structure makes it possible to study different layouts with minimal development work by the user; the flexibility implies possible application to different systems: from simple systems composed of a single gas turbine to hybrid systems including fuel cells (SOFC in particular).
Real-time execution capability allows on-line monitoring and verification during test rig operation.

MODEL LAYOUT

A previous study regarded the development of the entire RRFCS hybrid system [5][9]: the complete lay-out is shown in Figure 1. The availability of a pressurized SOFC test rig, representing a portion of the whole SOFC stack designed for the Figure 1 plant layout, motivated the development of a specific sub-system model.
Two important loops operate within such a sub-system:

- cathode (air) recycle;
- anode (fuel) recycle;

Fresh air flow from inlet is pre-heated by recycling a fraction of the cathode side exhausts. The recycle is driven by an ejector where high pressure primary air entrains hot secondary cathode exhaust [10].
On the anode side, a fraction of the steam rich stack off-gas is recycled into the incoming methane-based fuel to pre-heat the fuel itself and to carry out the steam methane reforming reaction, avoiding carbon deposition. The methane/steam mixture is then converted in a reforming rector into a hydrogen rich mixture, which is the actual fuel to the fuel cell. The recycle is driven also in this case by an ejector where primary fuel entrains the steam rich secondary fuel from stack outlet. Excess fuel discharged by the anode loop feeds the off-gas burner where it burns with air in the cathode recycle loop to help keeping the stack in temperature. The test rig and model layout is shown in Figure 2.

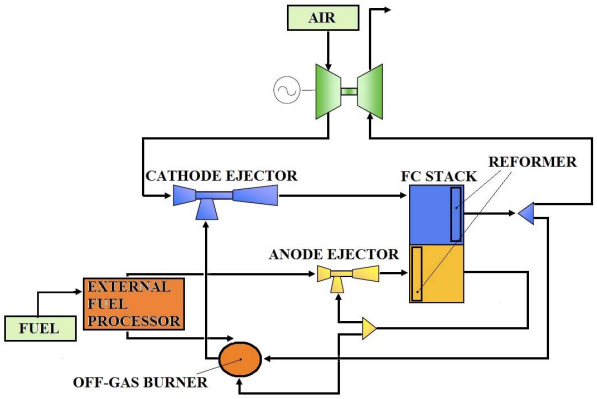

Figure 1 - Layout of the real-time hybrid system model

As can be inferred from Figures 1 and 2, the turbo machinery has been removed, while the ejectors are retained.

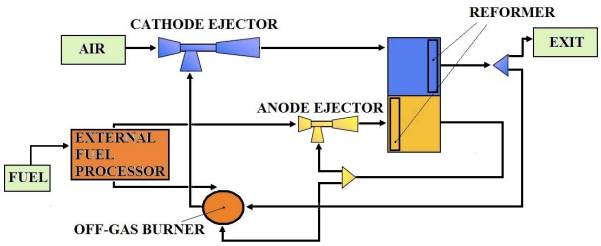

Figure 2 - Layout of the test-rig and real-time model

In this study the whole hybrid system model has been sized down to a single SOFC block level (about 15kWe power), representing the actual stack in the test rig. The single SOFC block is constituted by one "Reformer" and one "Stack". Cathode and anode ejector geometries were reduced accordingly.

REAL-TIME MODELLING

In late 2000, the Thermochemical Power Group (TPG) of Genoa University decided to develop the software named TRANSEO for the transient analysis of energy systems, based on MATLAB-Simulink environment [11]. TRANSEO has been used to study a variety of microturbine-based cycles, including SOFC hybrids [12][13][14].
Recently, TRANSEO components and the general approach have been modified to achieve real-time simulation capability [15], reducing computational efforts but slightly affecting accuracy.

The following main simplifications have been introduced:

i. when it is necessary to re-calculate flow thermo-physical properties, such as specific heat at combustor outlet, simple polynomial functions are used;

ii. component main functions have been translated from C language functions into embedded Matlab functions, characterized by a less time consuming execution;

iii. enthalpy balances are carried out with $C_p\Delta T$ approach to avoid the TRANSEO time consuming enthalpy calculation;

iv. iterative calculations for chemical reactions inside the cell are minimized. The component models have been simplified fixing the number of iterations at the minimum, without affecting stability performance and accepting an error under 1%;

v. component dimensions (for fluid dynamic delay only) have been increased through a multiplicative factor to have good stability using a step size of 0.01 seconds (the TRANSEO model uses a calculation step of 0.001 seconds). While this approach affects the calculation performance during the first part of simulation (the first seconds), the long time-scale phenomena are correctly calculated;

vi. continuous states have been substituted with discrete states in order to use the Simulink® fixed-step discrete solver.

Figure 3 shows the final structure of the modelled system.

As illustrated in Figure 3, the model inputs are as it follows:

- Anode_Fuel [m, p, T, c_p, R_g, LHV]: anode ejector fuel flow primary inlet;
- Syngas [m, p, T, cp, R_g, LHV]: additional fuel gas to the off-gas burner inlet;
- CellCurrent [A]: total electrical current drawn from the SOFC stack;
- Main_Air [m, p, T, c_p, R_g, LHV]: main air flow inlet;
- Vessel pressure [bar];

The model outputs are the following:

- OGB_outlet_Temp [K]: off-gas burner flow outlet temperature;
- CathEjector_out [m, p, T, c_p, R_g, LHV]: cathode ejector flow outlet temperature;
- Ref_out_Temp [K]: reformer cathode flow outlet temperature;
- IPV Outlet [m, p, T, c_p, R_g, LHV]: the hot exhaust exit;
- SingleBlock_Power [kW]: generated power;
- Stack_Outlet Temp [K]: stack anode flow outlet temperature.

The model is composed of the following subsystems: Cathodic_Loop, SOFC, Split_OGB_Turbine and OGB.
The *Cathodic_Loop* subsystem consists of (in series) a plenum, the cathode ejector and a pipe representing the pressure drop between cathode ejector and SOFC. The *SOFC* subsystem is represented in Figure 4 and it is the most complex, as it. He describes the interaction between anode ejector and SOFC, composed of reformer and stack.
The *Split_OGB_Turbine* splits cathode flow outlet between Turbine inlet and OGB inlet. In the actual rig the turbine is physically simulated by a calibrated orifice, which is reproduced in the model.
The *OGB* subsystem represents the anode off-gas burner behaviour.

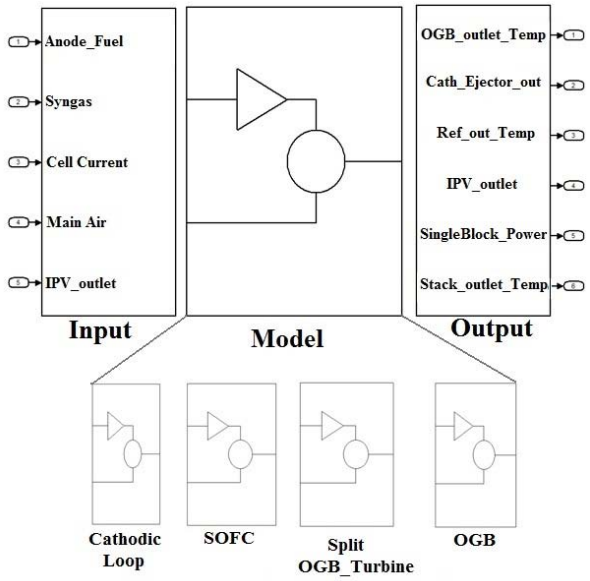

Figure 3 - Structure of the real-time model

SOFC and REFORMER BLOCK MODELS

The SOFC block model takes into account the planar geometry of the cell, which is assumed to be coupled to a reforming unit feeding the SOFC with a mixture of H_2, CH_4, CO, CO_2 and H_2O [16]. Chemical reactions such as shifting and methane reforming occur in the anodic compartment of the SOFC [17][18].

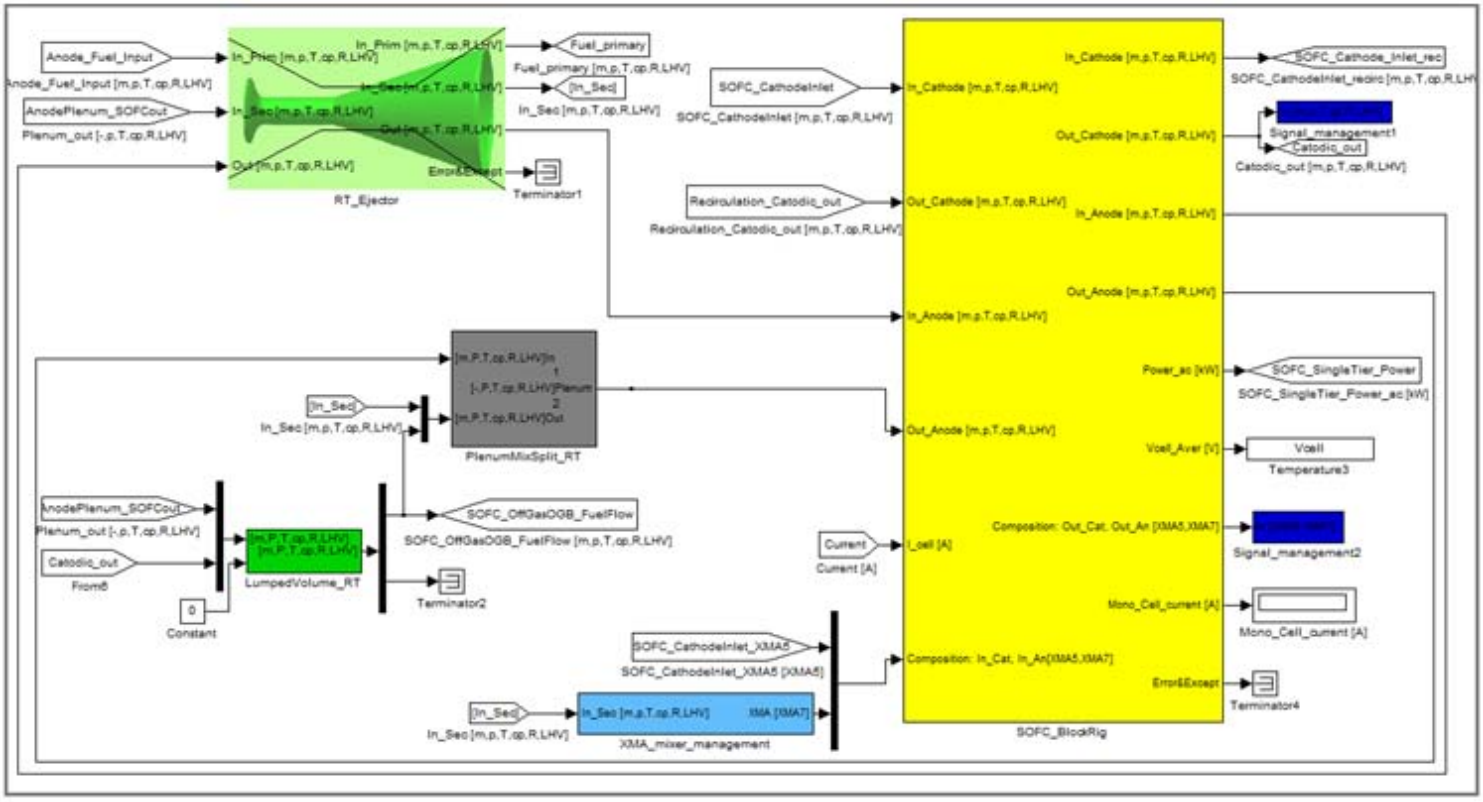

Figure 4 - SOFC subsystem

The main hypotheses of the model are:

- the cell is adiabatic;
- the cell voltage is uniform;
- all the chemical reactions within the anodic stream are at equilibrium;
- the electrochemical reaction of H_2 is taken into consideration while the electrochemical reaction of CO is neglected.

The cell model includes:

- electrochemical performance: the current-voltage behaviour of the stack is evaluated by subtracting the overall voltage losses from the thermodynamic potential (i.e. the voltage of the stack under conditions of thermodynamic reversibility), see Eq. 1-8;

$$V_{oc} = -\frac{\Delta G}{2F} = -\frac{\Delta G^0}{2F} + \frac{RT}{2F} ln \frac{p_{H2} \cdot (p_{O2})^{1/2}}{p_{H_2O}} \quad (1)$$

$$\Omega_t = \sum \Omega_{ohm} + \sum \Omega_{att} + \Omega_{dif} \quad (2)$$

Where Ω_{dif} is defined as the difference between thermodynamic open circuit potential calculated for undisturbed flow and the one calculated within reaction site.

$$\rho_{el} = A_{\mathrm{el}} \exp\left(-\frac{B_{\mathrm{el}}}{T}\right) \quad (3)$$

$$\rho_c = A_c \exp\left(-\frac{B_c}{T}\right) \quad (4)$$

$$\rho_c = A_c \exp\left(-\frac{B_c}{T}\right) \quad (5)$$

$$\frac{1}{\Omega_{act,a}} = D_1 \frac{2F}{R_g T} \cdot \left(\frac{p_{H2}}{p^o}\right)^{m_1} e^{-(\mathrm{E}_a/RT)} \quad (6)$$

$$\frac{1}{\Omega_{act,c}} = D_2 \frac{2F}{R_g T} \cdot \left(\frac{p_{H2}}{p^o}\right)^{m_2} e^{-(\mathrm{E}_c/RT)} \quad (7)$$

Equation 2 shows the total electrical resistance as a sum of ohmic, activation and diffusion resistances based on the relative resistivities calculated by Eqs. 3-7, the total cell power is defined by Eq. 8;

$$P = (V_{oc} + \Omega_t I) \bullet I \quad (8)$$

- equilibrium of reforming and shifting chemical reactions (Eqs. 9-10);

$$K_{p,ref} = \frac{p_{H_2}^3 p_{CO}}{p_{CH_4} p_{H_2O}} \text{ reforming} \quad (9)$$

$$K_{p,shift} = \frac{p_{CO_2} p_{H_2}}{p_{CO} p_{H_2O}} \text{ shifting} \quad (10)$$

- energy balances of gaseous flows;
- mass balances of anodic and cathodic flows.

In the Stack Model the electrical current-voltage performance is evaluated on the basis of the average values of the physical-chemical variables. The other equations are in the form of macroscopic balances, they simply express a balance between inlet and outlet flows of mass and energy, and allow the evaluation of the average values only of the physical-chemical variables within the electrochemical reactor.

With comparison to the original hybrid system model [11], the stack model was modified from the entire hybrid system (Figure 1) to the actual test rig layout and size (Figure 2) involving the following updates of the input data:

- reduction in the surface area of each cell;
- update of the number of cells in a tube;
- update of the number of tubes in a bundle;
- update of the number of bundles in a strip;
- update of the number of strips in a block.

On the other hand, the correlation for voltage losses have been retained, even if the stack has experimentally shown improved performance: a conservative approach was decided at this stage.
In the TRANSEO model the reformer is represented with ten calculation nodes; in the real-time model the reformer is simulated with only one calculation node, which includes the whole active surface for catalysis and heat transfer. For this reason, the output composition has been assumed to be at the chemical equilibrium, being representative of the experimental evidence.
The reforming reaction considered is the steam methane reforming process, Eq. (11). This reaction is assumed at equilibrium together with the shifting reaction, Eq. (12). The equilibrium constants are derived as a function of temperature from Gibbs energy minimization.

$$CH_4+H_2O \rightarrow 3H_2+CO \qquad \Delta H = 206 \text{ MJ/kmol} \quad (11)$$

$$CO+H_2O \rightarrow CO_2 + H_2 \qquad \Delta H = -41 \text{ MJ/kmol} \quad (12)$$

Since the reforming reaction is overall endothermic, the thermal flow exchanged from the cathode side to the anode side in the reformer is calculated throughout equations (13) and (16): properties refer to the cathode side. The temperature at the anode fuel gas output is considered to be identical to $T_{sol_{av}}$.

$$\mathrm{Nu} = 4 \quad (13)$$

$$h_{re} = \frac{(Nu \cdot k_{re})}{hd_{re}} \quad (14)$$

$$Q_{re} = h_{re} \cdot S_{re} \cdot (T_{c_{av}} - T_{sol_{av}}) \quad (15)$$

$$c_{re} \cdot M_{re} \frac{d(T_{sol_{av}})}{dt} = Q_{re} \quad (16)$$

EJECTOR SIZING

After updating the cell model, it was necessary to update the following ejector geometrical data:

- Nozzle length
- Nozzle outlet diameter
- Mixing diameter
- Diffuser outlet diameter
- Diffuser opening angle
- Total length

The model settings have been adjusted to meet the specifications of the RRFCS system.

EXPERIMENTAL VALIDATION

In mid 2009 RRFCS carried out an important experimental campaign to test the performance of the system layout presented above. This campaign produced a set of data that could be used for model validation.
The first evaluation of the model behaviour was carried out at constant inputs. Figure 5 shows the evolution of the main inputs along the entire test: validation was performed in a time window of about two hours, between approximately 60000s and 68000s.
The red circle in the charts indicates approximately the time interval in which the real-time model was validated.
Figure 6 shows the zoom of the model inputs around the validation time window: in the first 2500s of such an interval the inputs are constant; then steps are applied and transient behavior is tracked by measurements.
With reference to Figure 6, the main input variations happen in the following sequence:

1. SOFC current step, time = 62100 [s]
2. SOFC main fuel step, time = 62100 [s]
3. Main air double steps, start time = 63200 [s];
4. SOFC main fuel step, time = 63300 [s];

Main air temperature and pressure vary as a consequence of the main air flow variation: since this is due to the electrical heater and the air plenum, not included in the model, they have been assumed as model inputs. OGB additional syngas flow is controlled by a temperature-based controller in the actual test rig: such a controller is not present in the model, so the OGB syngas fuel is used as an input as well.

In the performance analysis the following parameters were evaluated:

- Temperatures at cathode and anode ejector flow primary inlets, secondary inlets and outlets;
- Temperatures at stack anode and cathode inlets and outlets;
- Temperatures at reformer anode and cathode outlets.

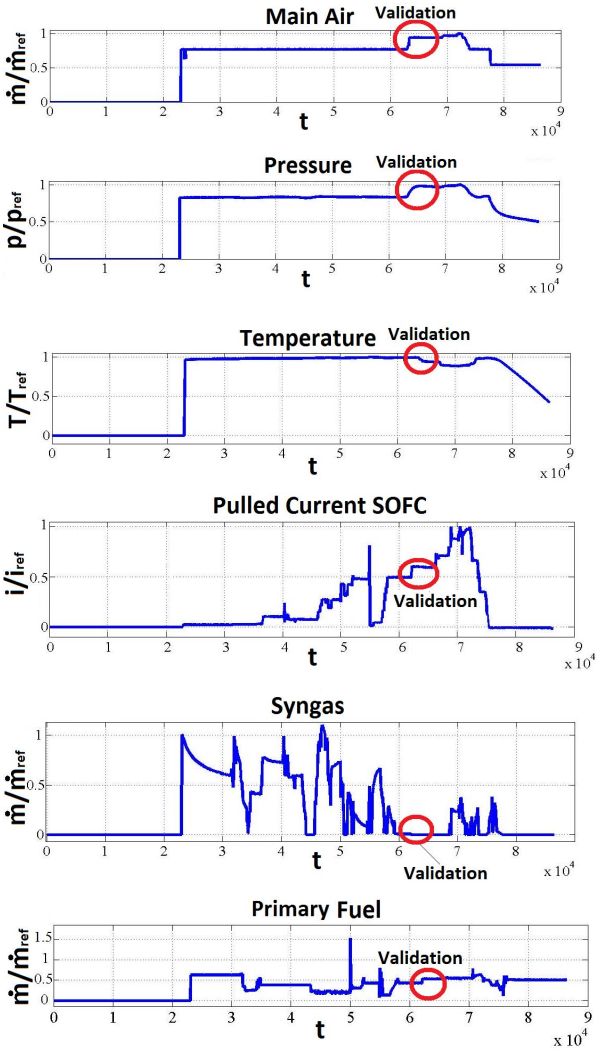

Figure 5 - The experimental data input to the model

A first simulation was performed, showing a few details that were not accurate enough: results from this first simulation are not reported. At steady-state the temperatures were a few tens of degrees different from the experimental data. The main reason was found to be in the heat losses, which were ignored: appropriate thermal considerations about stack and system features made it possible to better estimate them. As a result, heat losses accounted for about 10% of the thermal input, this being justified by the experimental character of the installation, which was not optimized for performance.

Another inaccuracy was in the cathode ejector flow, due to underestimation of the pressure losses: when the measured value, in the order of some tens of mbar, was used, then the predicted recirculation factor (and temperatures as a result) showed a better ordinance to experiment.

After this first phase of improvement the gap between modelled and experimental data was reduced significantly at steady-state.

At this point, a second simulation was performed, focusing on the transient operation and prediction of trends.

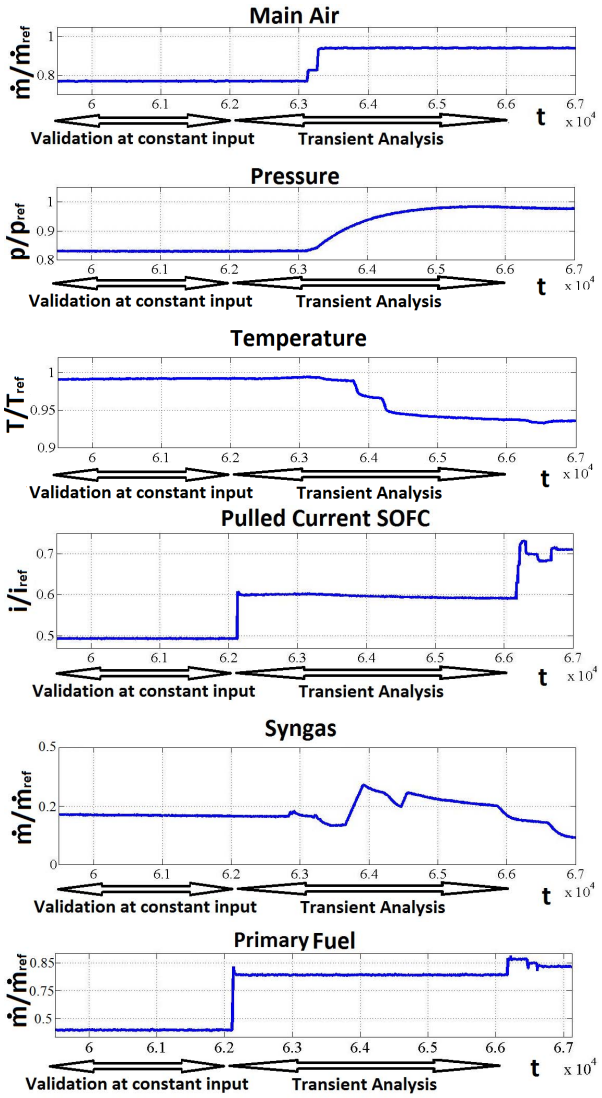

Figure 6 - Experimental data: zoom in the validation interval

The model results were compared to experimental data. In the comparison of temperatures, percentage values were considered to be more meaningful than absolute values: in fact, 10K difference, apparently significant at ambient conditions, becomes acceptable at 1100K, which represents the average operating conditions of the SOFC stack. Predictions of curves were also compared using non-dimensional temperatures.

At this point, some discrepancies between simulated and measured data were still observed.

Figure 7 shows the curve of the predicted cathode ejector outlet temperature.

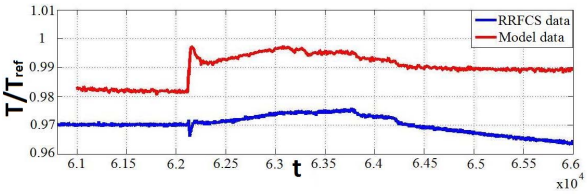

Figure 7 - Temperature at Cathode Ejector outlet in the second simulation

In the initial and later time intervals, the model followed the experimental data trend faithfully: however, when the steps in the inputs were applied, the model showed a rapid temperature rise, which contradicts the experimental evidence of a temperature dip. Without such an offset, the final predicted temperature would have been much closer to the experimental value. To understand the reason for such very different behaviour, the experimental temperature was introduced as an input in the cathode ejector flow outlet and the entire model was simulated. In this way all temperatures followed the measured trend: so, this was helpful in identifying the problem in the OGB outlet temperature. OGB temperature rise is due both to the anode off-gases and the additional syngas, which is fed so as to have direct control of the thermal management of the test rig. The syngas flow was an input to the model, thus the problem had to derive from the predicted anode off-gas flow from the SOFC stack (not measured in the rig). As shown in Figure 8, the anode off-gas fuel flow to the OGB inlet has a clear correlation with the cathode outlet temperature curve.

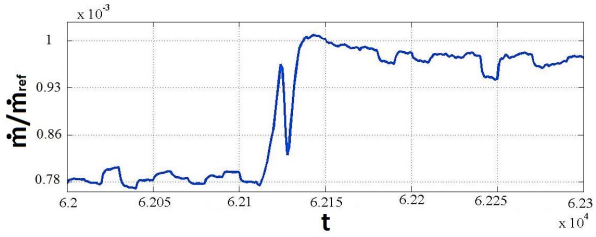

Figure 8 - Fuel flow at OGB inlet in the second simulation

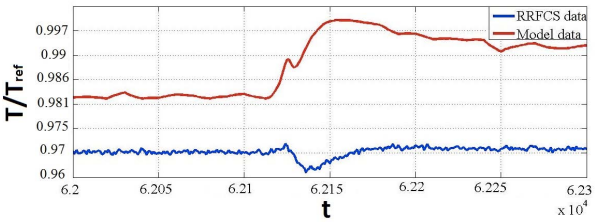

Figure 9 - Zoom on temperature at Cathode Ejector outlet in the second simulation

The reason for the temperature dip in the experimental data can be found in the reformer: in the short time when additional fuel is sent to the stack following the additional current drawn, the fastest effect is a temperature drop in the reformer, which, because of system layout (Figure 2), is immediately fed back to the cathode ejector secondary flow and outlet flow. In the model, this effect was present (as later shown in Figure 13); the problem was that the anode volume was not simulated (i.e. anode pressurization was not considered a significant phenomenon to be represented). As a result, the increase in current caused a sudden increase in the oxygen ions transported to the anode side, and thus a sudden increase of the anode outlet flow and, as a consequence, a sudden increase in the anode off-gases sent to the OGB. The solutions to this problem could be twofold: to include a plenum for simulating the anode volume on the anode side, or to simply introduce a time delay in the anode off-gases sent to the OGB. The latter was the solution implemented given the real-time oriented modelling approach.

The final simulation provided the results shown in the following Figures 10 to 15.

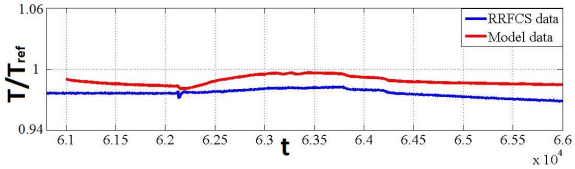

Figure 10 - Temperature at Cathode Ejector outlet

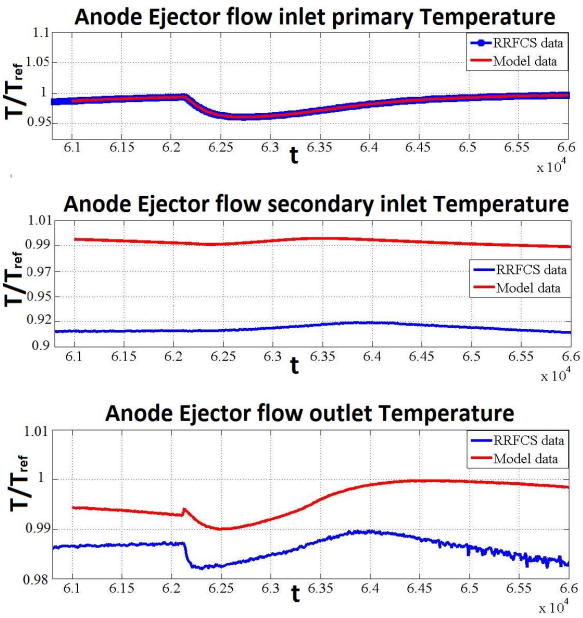

Figure 11 - Anode Ejector

In the final simulation, both ejectors presented a good accuracy in predicting the behaviour of the temperature: a small discrepancy was still visible in the anode ejector outlet (Figure 11), but since it was limited to a couple of degrees K, it was considered to be acceptable.

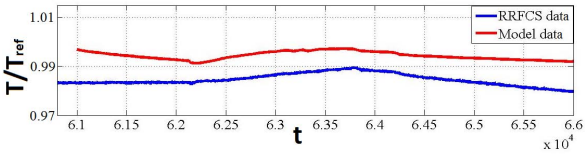

Figure 12 - Temperature at Stack Cathode inlet

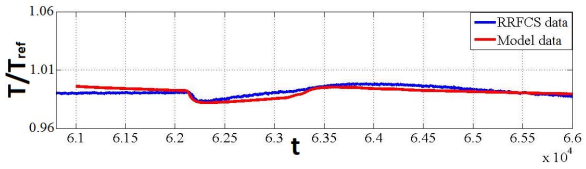

Figure 13 - Temperature at Reformer Cathode outlet

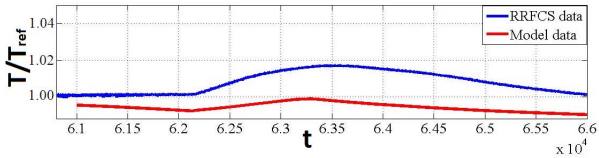

Figure 14 - Temperature at Stack Cathode outlet

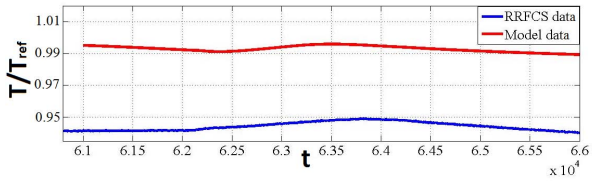

Figure 15 - Temperature at Stack Anode outlet

In general, it can be observed that:

- Stack anode and cathode inlet temperature are higher than experimental data;
- Stack anode and cathode outlet temperatures are lower than experimental data;
- The real-time stack model is therefore apparently more efficient than the one under test. This was confirmed by RRFCS personnel: the stack which was the subject of this experimental campaign was a beta version, showing higher area specific resistance (ASR) than expected. This has been resolved in later tests.

All temperatures in the final simulation fitted the experimental data well, apart from the stack anode outlet (Figure 15): the temperature gap between the measured and the simulated ones is about 40 K. This was subject of further investigation: on analyzing the experimental set-up, it was concluded that the thermocouple for such a temperature was not positioned correctly, as it was measuring the off-gas temperatures after a considerable length of piping, which could cause a significant temperature drop. So this explained why the predicted temperature was higher than the measured one. This conclusion also helped in redesigning the position of this thermocouple, so as to improve the accuracy of future testing at the stack anode outlet.
This final result also makes it possible to highlight another additional value in dynamic modelling: checking for possible problems in the experimental set-up, thus providing useful feedback for design improvements.

CONCLUSIONS

The primary aim of this study was to set up and validate a real-time dynamic model of a new test facility developed and operated by RRFCS, to test individual SOFC blocks. Validation of dynamic models is a fundamental step in assessing their reliability and accuracy. In the future, the model could be used to interact with the actual rig, in order to monitor non-measured properties and ensure safe operation of the stack.
Despite of the complexity of the model, including very different components (fuel cell stack, reformer, burner, ejectors), it presents good computational performance (real-time applications are possible) and acceptable prediction accuracy, both at steady-state and transient conditions.
Since this is a validation analysis on temperatures, the deviation between predicted and measured values can be quantified as follows:

- The maximum error on stack cathode inlet temperature is 1.6%;
- The average deviation between measured and predicted stack cathode inlet temperatures is 9.7 K;
- The maximum error on the stack cathode outlet temperature is 2.1%;
- The average deviation between measured and predicted stack cathode inlet temperature is 13.9 K;

Such deviations quantify the accuracy of the model.

ACKNOWLEDGEMENTS

The authors wish to thank Rolls-Royce Fuel Cell Systems Limited for the data provided.

REFERENCES

[1] M. Fardadi, F Muller, F. Jabbari, 2010, “Feedback control of solid oxide fuel cell spatial temperature variation”, Journal of Power Source, Vol. 19, Issue 13, pp. 4222-4223.

[2] J. Milewski,A. Miller, A. Dmowski, P. Biczel, 2009, “Methodology for the control strategy for a solid oxide fuel cell hybrid system”, Archives of Thermodynamics Vol. 30, No. 4, pp. 25-44.

[3] A. Tsai, L. Banta, L. Lawson, D. Tucker, 2009, “Determination of an Empirical Transfer Function of a Solid Oxide Fuel Cell Gas Turbine Hybrid System Via Frequency Response Analysis“, Journal of Fuel Cell Science and Technology, Vol. 6 (3), pp. 034505.

[4] A.F. Massardo, L. Magistri, 2003, "Internal reforming solid oxide fuel cell gas turbine

combined cycles (IRSOFC-GT) - Part II: Exergy and thermoeconomic analyses", Journal of Engineering for Gas Turbines and Power, Vol.125(1), pp. 67-74

[5] F. Trasino, M. Bozzolo, L. Magistri, A. F. Massardo, 2011, "Modeling and Performance Analysis of the Rolls-Royce Fuel Cell Systems Limited: 1 MW Plant", J. Eng. Gas Turbines Power, Vol.133(2), 021701.

[6] D. K. Nichols, G. Agnew, D. Strickland, 2008, "Outlook and Application Status of the Rolls Royce Fuel Cell System SOFC", PES General Meeting, Pittsburgh, Pennsylvania (USA).

[7] F. Zabihian, A. Fung, 2009, "A Review on Modeling of Hybrid Solid Oxide Fuel Cell Systems", International Journal of Engineering (IJE), Vol. 3(2), pp.85-119.

[8] F. Mueller, R. Gaynor, A. E. Auld, J. Brouwer, F. Jabbari, G.S. Samuelsen, 2008, ``Synergistic integration of a gas turbine and solid oxide fuel cell for improved transient capability," Journal of Power Sources , Vol. 176, pp 229.

[9] G. Agnew, R. D. Collins, M. Jorger, S. H. Pyke, R.P. Travis, 2007, "The Components of a Rolls-Royce 1MW SOFC System", 10th International Symposium on Solid Oxide Fuel Cells (SOFC-X), Vol. 7, Issue , pp. 105-111.

[10] M. L. Ferrari, D. Bernardi, A. F. Massardo, 2006, "Design and testing of ejectors for high temperature fuel cell hybrid systems", Journal of Fuel Cell Science and Technology, Vol. 3(3), pp.284-291

[11] A. Traverso, 2005, "TRANSEO code for the dynamic performance simulation of micro gas turbine cycles", ASME Paper GT2005-68101.

[12] A. Ferretti, A. Traverso, A. F. Massardo, G. Saunders, 2010, "Transient model validation of a syngas generator for SOFC systems", ASME Paper ICEPAG2010-3436.

[13] M. L. Ferrari, M. Pascenti, A. F. Massardo, 2008, "Ejector Model for High Temperature Fuel Cell Hybrid Systems: Experimental Validation at Steady-State and Dynamic Conditions", *Journal of Fuel Cell Science and Technology*, Vol. 5, 041005, 1-7.

[14] M. L. Ferrari, E. Liese , D. Tucker, L. Lawson, A. Traverso, A.F. Massardo, 2007, "Transient Modeling of the NETL Hybrid Fuel Cell/Gas Turbine Facility and Experimental Validation", *Journal of Engineering for Gas Turbines and Power*, Vol. 129, pp. 1012-1019.

[15] F. Ghigliazza, A. Traverso, A. F. Massardo, J. Wingate, M.L. Ferrari, 2009,"Generic Real-Time Modeling of Solid Oxide Fuel Cell Hybrid Systems", *Journal of Fuel Cell Science and Technology*, Vol. 6 / 021312-1.

[16] A. F. Massardo, F. Lubelli, 2000, "Internal Reforming Solid Oxide Fuel Cell - Gas Turbine Combined Cycles (IRSOFC-GT). Part A: Cell Model and Cycle Thermodynamic Analysis", ASME Transactions, Journal of Engineering for Gas Turbines and Power, January 2000, Vol. 122, pp. 27-35

[17] S.H. Chan, H.K. Ho, Y.Tian, 2002, "Modeling of simple hybrid solid oxide fuel cell and gas turbine power plant", Journal of Power Sources, Vol 109, pp. 111-120

[18] J. VanOsdol, E. Liese, D. Tucker, R. Gemmen, R. James, 2010, "Scaling a Solid Oxide Fuel Cell Gas Turbine Hybrid System to Meet a Range of Power Demand", Journal of Fuel Cell Science and Technology, Vol. 7 (1), pp. 015001.